Environmental Science & Technology

Article

Cite This: Environ. Sci. Technol. 2018, 52, 5812−5820

pubs.acs.org/est

Facile On-Site Aqueous Pollutant Monitoring Using a Flexible, Ultralight, and Robust Surface-Enhanced Raman Spectroscopy Substrate: Interface Self-Assembly of Au@Ag Nanocubes on a Polyvinyl Chloride Template

Lu-Bin Zhong,[†,‡] Qing Liu,[†,§] Peng Wu,[†] Qi-Feng Niu,[†] Huan Zhang,[†,§] and Yu-Ming Zheng*[,†,‡]

[†]CAS Key Laboratory of Urban Pollutant Conversion, Institute of Urban Environment, Chinese Academy of Sciences, 1799 Jimei Road, Xiamen 361021, P. R. China

[‡]CAS Center for Excellence in Regional Atmospheric Environment, Institute of Urban Environment, Chinese Academy of Sciences, 1799 Jimei Road, Xiamen 361021, P. R. China

[§]University of Chinese Academy of Sciences, 19A Yuquan Road, Beijing 100049, P. R. China

Supporting Information

ABSTRACT: Aquatic ecosystems and human health have been seriously threatened by illegal discharge of wastewater, while simple and effective monitoring methods are still sparse. Here, we propose a facile method for on-site pollutant monitoring by surface-enhanced Raman spectroscopy with a novel substrate. This substrate is fabricated by interface self-assembly of Au@Ag nanocubes (NCs) on a simultaneously formed polyvinyl chloride (PVC) template, followed by coating with a thin Au film. The Au@Ag@Au-NCs/PVC film is flexible, ultralight, and robust and could float on the surface of water and firmly contact with water even under harsh environmental conditions. Moreover, the Au@Ag@Au-NCs/PVC film is translucent, allowing penetration of laser beams and enhancement of Raman signals. When thiram was used as a model contaminant in aqueous solution, a good linear relationship (R^2 = 0.972) was obtained over the range of 0.1−50 ppb with a detection limit of 0.1 ppb. Raman signals of thiram can be instantly and consecutively detected with the enhancement of the film in the simulated experiments, suggesting its possible use in the long run. Furthermore, the film can be easily regenerated by $NaBH_4$ solution washing, which could reduce the operating cost. In summary, the Au@Ag@Au-NCs/PVC film has great potential in on-site pollutant monitoring in aqueous environments with a portable Raman spectrometer.

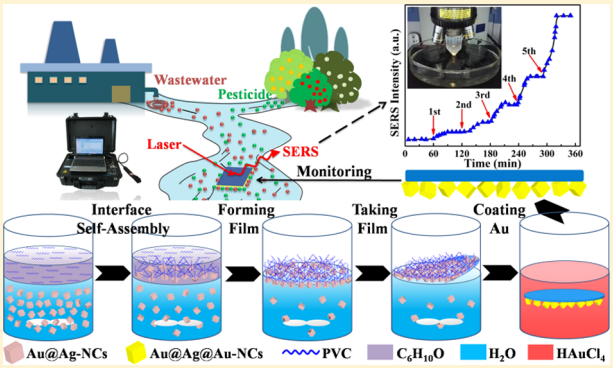

1. INTRODUCTION

Water is the most important and essential substance for life in this world. Meanwhile, providing clean and safe drinking water has become a tremendous challenge due to the growth of population, rapid industrialization, and increasing agricultural activities.[1,2] Nowadays more than 1.2 billion people face a lack of safe drinking water, while 3900 children die every day due to diseases caused by unsafe water sources.[2,3] Illegal discharge of hazardous chemicals is a major cause of water quality deterioration.[4−6] It is reported that up to 80% of untreated sewage is discharged directly into the water in developing countries.[4] Furthermore, illegal discharge often occurs randomly, causing difficulty in immediate response and mitigation.[4] Therefore, development of effective and economical methods for on-site contaminant monitoring in natural water bodies is of great significance and necessity.

To date, various analytical techniques have been developed to detect contaminants in water, including UV−vis spectroscopy, fluorescence spectroscopy, immunoassays, high-performance liquid chromatography coupled with mass spectroscopy (HPLC-MS), gas chromatography coupled with mass spectroscopy (GC-MS), and capillary electrochromatography combined with UV laser-induced fluorescence.[7,8] Unfortunately, most of these analytical procedures require expensive instruments, tedious sample pretreatment, or skilled workers with a high level of analytical expertise and, thus, are not suitable to be performed on-site,[9,10] leaving loopholes for illegal discharge. Hence, on-site aqueous contaminant monitoring is still a great challenge.

Due to its unique merits, such as rapid, ultrasensitive, distinctive fingerprinting, nondestructive analysis, and negligible

Received: September 8, 2017
Revised: February 28, 2018
Accepted: April 16, 2018
Published: April 16, 2018

DOI: 10.1021/acs.est.7b04327
Environ. Sci. Technol. 2018, 52, 5812−5820

Scheme 1. Preparation of the Au@Ag@Au-NCs/PVC Film and Its Application As a SERS Substrate for On-Site Monitoring of Contaminants in Water Bodies

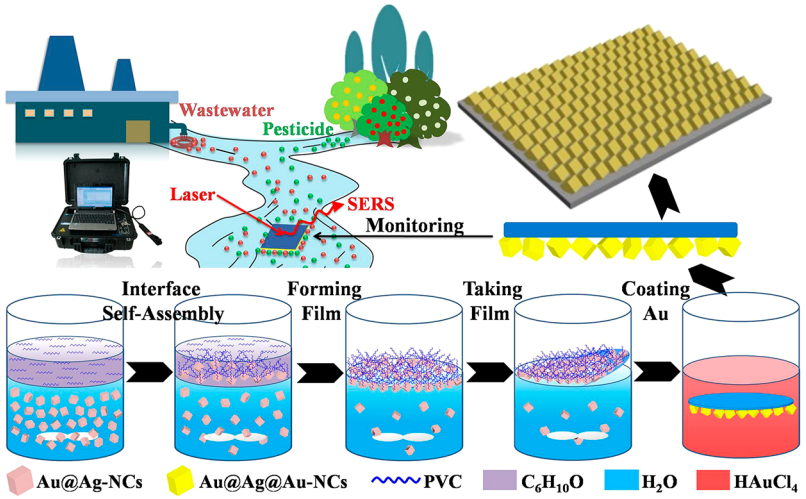

interference by water, the surface-enhanced Raman scattering (SERS) technique has attracted great attention and become a powerful analytical technique in biomedicine, food safety, and environmental monitoring.[10−13] SERS substrates, which can greatly amplify Raman scattering signals to achieve high sensitivity, are critical in SERS measurement.[14,15] Currently, metal nanoparticle (NP) colloids and well-ordered metal nanostructures are two types of typical SERS substrates.[11] Metal NP colloids have a relatively simple preparation process, but the uncontrollable aggregation of NP colloids often leads to poor reproducibility.[16] Well-ordered metal nanostructures can improve the reproducibility of SERS analysis; however, most of the nanostructures are fabricated on hard templates, such as glass, quartz, or silicon, by weak physical adsorption or electrostatic interaction. Therefore, these substrates are rigid and heavy, which are not versatile enough for practical application.[17] Furthermore, the assembled nanostructures are prone to destruction under external force, for example, by friction, ultrasound, or chemical washing. In addition, for both SERS substrates, preparing and dropping liquid samples on the substrate is needed for the detection. Therefore, ceaseless sampling, which is rather tedious, is necessary to achieve on-site monitoring of aqueous pollutants via existing SERS methods. To overcome these drawbacks, a novel SERS substrate, which can avoid ceaseless sampling and offer on-site monitoring of aqueous contaminants, is urgently needed.

Recently, we developed a novel flexible SERS substrate with assembled gold nanoparticles (Au-NPs) on newborn poly(methyl methacrylate) (PMMA) template by interface self-assembly method.[18] The fabricated Au-NPs/PMMA SERS substrate was flexible, ultralight, and translucent. The distinct advantages of this novel substrate are that no sampling is needed in the SERS detection and an irregular surface can be tested. Thus, the Au-NPs/PMMA substrate is highly versatile and can be used in various conditions. However, as the PMMA template is relatively weak, polyethylene (PE) film is required to support the Au-NPs/PMMA substrate. Also, the substrate may be peeled off from PE film during a long-term detection. In addition, ethanol is necessary to induce self-assembly of Au-NPs, making the preparation procedure rather tedious.[18−20] Hence, further improvement on the present Au-NPs/PMMA substrate is necessary to ensure on-site monitoring of aqueous contaminants.

In this work, we developed a simpler method to fabricate a lighter, stronger, and more flexible and robust SERS substrate. First, a stronger polymer, polyvinyl chloride (PVC), is chosen to replace the PE film and PMMA, as it can fix and support the self-assembled NPs. Next, cyclohexanone, which is a better solvent for PVC, is used instead of toluene. More importantly, ethanol, the inducer, is removed as the PVC cyclohexanone solution can directly induce the rise and assembly of NPs (Figure S1). Hence, the overall preparation process of the Au@Ag@Au-NCs/PVC film is simplified and the cost is reduced, as shown in Scheme 1. As the film is light and can float on the surface of water, on-site SERS monitoring for illegal discharge is feasible by a portable Raman spectrometer (Scheme 1). Thiram is used as the model contaminant in standard water solution and actual aqueous samples, and the detection limits were determined to be 0.1 and 1 ppb, respectively. In addition, the Au@Ag@Au-NCs/PVC film also demonstrates its feasibility in extremely harsh environmental conditions. Simulated experiments show that the Au@Ag@Au-NCs/PVC film can capture sudden spikes in thiram concentration and, thus, is suitable for illegal discharge detection and monitoring.

2. MATERIALS AND METHODS

2.1. Materials. Hydrogen tetrachloroaurate (III) trihydrate ($HAuCl_4 \cdot 3H_2O$, 99.9%), sodium borohydride ($NaBH_4$, 99%), L-ascorbic acid (AA, >99%), silver nitrate ($AgNO_3$, >99%), cetyltrimethylammonium bromide (CTAB, 99%), ethanol (C_2H_6O, 99%), and Malachite Green (MG, $C_{23}H_{25}ClN_2$) were purchased from Sinopharm Chemical Reagent Co. Ltd. (Shanghai, China). Thiram ($C_6H_{12}N_2S5$, 97%), cyclohexanone ($C_6H_{10}O$, 99%), and parathion-methyl solution ($C_8H_{10}NO_5PS$) were obtained from Aladdin Chemical Reagent Co. Ltd. (China). Cetyltrimethylammonium chloride (CTAC) solution, 4-aminothiophenol (4-ATP, C_6H_7NS, 97%), and polyvinyl chloride (PVC, Mw 1.2×10^5) were purchased from Sigma-Aldrich. Estuary water and secondary effluent were taken directly from Xinglin Bay at Xiamen City and a local wastewater treatment plant (WWTP), respectively. Milli-Q water was used throughout the study.

DOI: 10.1021/acs.est.7b04327
Environ. Sci. Technol. 2018, 52, 5812−5820

2.2. Synthesis of CTAC-Capped Au-NPs. Au-NPs were prepared using the seed-mediated growth method. First, a brownish seed solution was prepared by adding ice cold $NaBH_4$ (0.6 mL, 0.01 M) into a 10 mL aqueous solution containing $HAuCl_4$ (0.25 mM) and CTAB (0.1 mM). The seed solution was then aged at 27 °C for 3 h. Next, a growth solution was prepared by mixing $HAuCl_4$ (6 mL, 0.5 mM), CTAC (6 mL, 0.2 M), and AA (4.5 mL, 0.1 M). A 0.3 mL portion of the as-prepared seed solution was then added into the above growth solution, and the reaction mixture was gently mixed for 30 s and left undisturbed for 30 min. The final solution was purified by centrifuging at 12 000 rpm for 25 min and redispersed into Milli-Q water.

2.3. Fabrication of Au@Ag Nanocubes (Au@Ag-NCs). Au@Ag-NCs were prepared by the seed-mediated method, as reported by Xia et al. with slight modifications.[21] First, 0.5 mL of the above Au-NPs solution was mixed with 18 mL of CTAC (20 mM) aqueous solution in a 100 mL glass vial and heated at 60 °C for 20 min under magnetic stirring. Then, 20 mL of $AgNO_3$ solution (2 mM) and 20 mL of AA-CTAC solution (containing 50 mM AA and 40 mM CTAC) were simultaneously injected into the above solution at a rate of 0.2 mL/min using a syringe pump, while the reaction mixture turned from red to brownish-yellow. After 4 h, the vials were cooled in an ice-bath. The products were collected by centrifugation (12 000 rpm for 15 min), and then washed with Milli-Q water. The mean size of the as-prepared Au@Ag-NCs was 50 ± 5 nm.

2.4. Preparation of the Au@Ag@Au-NCs/PVC Film. First, 15 mL of freshly prepared Au@Ag-NCs suspension was transferred into a beaker, followed by addition of 3 mL of cyclohexanone with desired concentration of PVC. Due to the immiscibility of water and cyclohexanone, a clear water/cyclohexanone interface was formed. After that, the mixed solution was gently stirred by a magnetic rotator, and the Au@Ag-NCs gradually rose up to the water−cyclohexanone interface and self-assembled into orderly Au@Ag-NCs layers. A thin PVC template was simultaneously formed on the aqueous solution surface due to the evaporation of cyclohexanone. The self-assembled Au@Ag-NCs layers were then fixed by the newborn PVC template. When the cyclohexanone fully evaporated, the Au@Ag-NCs/PVC film formed and was retrieved from the solution surface.

Next, the Au@Ag-NCs/PVC film was dipped into 0.1 mM $HAuCl_4$ solution for 30 s to coat a thin Au-film on the Au@Ag-NCs surface. Finally, the Au@Ag@Au-NCs/PVC film was obtained.[22,23] The as-prepared film was treated in oxygen plasma (PDC-002, Mycro, USA) to strip away the redundant PVC on the Au@Ag@Au-NCs layer and was further washed by $NaBH_4$ solution and Milli-Q water. For ease of comparison, the Au@Ag@Au-NCs/PVC film was cut into squares of 0.5 cm × 0.5 cm, which were used as SERS substrates in the subsequent experiments. Assembling Au@Ag-NCs layers on glass was also fabricated for comparison. The preparation procedure was similar to that for the Au@Ag@Au-NCs/PVC film, except that ethanol was added and glass was used as a carrier instead of PVC to support the assembled Au@Ag-NCs layers, as previously reported.[19]

2.5. Preparation of SERS Samples. To determine SERS enhancement factor and reproducibility of the as-obtained Au@Ag@Au-NCs/PVC film, SERS sample 1 was prepared as follows. First, the Au@Ag@Au-NCs/PVC film was immersed in a 10^{-4} M 4-ATP ethanol solution for 30 min. Then, the Au@Ag@Au-NCs/PVC film was rinsed with ethanol to remove the unbound 4-ATP molecules and dried at room temperature to evaporate the residual ethanol.

To evaluate the applicability of the Au@Ag@Au-NCs/PVC film as a SERS substrate for aqueous contaminant detection, SERS sample 2 was prepared. Briefly, 100 ppm thiram solution in ethanol was prepared, and then diluted with Milli-Q water to the predetermined concentration in a flask. Then, a piece of Au@Ag@Au-NCs/PVC film was placed on the thiram water solution surface, with the exposed side of Au@Ag@Au-NCs attaching the water surface. Then, the flask was shaken at 200 rpm and 25 °C for 12 h.

Simulated on-site pollutant monitoring experiment using the Au@Ag@Au-NCs/PVC film was also conducted. A 200 mL portion of ultrapure water in the Petri dish represents an uncontaminated river at the beginning of the experiment, while SERS signals of the as-obtained Au@Ag@Au-NCs/PVC film were collected. After 60 min, a spike of thiram solution (40 μL, 10 ppm), representing sudden illegal discharge, was injected near the film location to better present the practical scenario, that is, the monitoring setup would be installed near the effluent discharge pipes. A 60 min period after the first injection, a second spike thiram solution was injected, which represents another illegal discharge. The process was then repeated five times. Meanwhile, the Raman signals of the film were continuously collected. A similar simulation experiment using estuary water from Xinglin Bay was also carried out using a portable Raman spectrometer on-site.

2.6. Characterization and SERS Analysis. Optical characterization was carried out by a UV−vis spectrophotometer (UV-759, Puxi, China). SEM images were acquired using a field-emission scanning electron microscope (FE-SEM) (Hitachi S-4800, Japan). Transmission electron microscope (TEM) images were obtained using a Philips Tecnai F30 (FEI, USA) operated at 300 kV. Mechanical strength of the Au@Ag@Au-NCs/PVC film was evaluated using a universal tensile machine (AGS-X, Shimadzu, Japan). The XPS spectra were acquired using a Thermo Fisher ESCALAB 250Xi spectrometer with a 150 W monochromatic Al Kα source. SERS spectra were acquired using a confocal microscope Raman spectrometer (LabRAM Aramis, France) with a 50× objective (Leica) and a numerical aperture of 0.55. Laser with a wavelength of 633 nm was used for Raman excitation, which was focused onto a sample with a spot size of approximately 2 μm^2. A portable Raman spectrometer (Advantage Raman Series, DeltaNu) was deployed for on-site pollutant monitoring.

3. RESULTS AND DISCUSSION

3.1. Preparation of the Au@Ag@Au-NCs/PVC Film. The fabrication process of the Au@Ag@Au-NCs/PVC film is shown in Scheme 1. Generally, an organic solvent−water interface is formed with a lower layer of Au@Ag-NCs aqueous solution and an upper layer of PVC cyclohexanone solution. PVC is chosen to form a template to fix and support the self-assembled Au@Ag-NCs due to its high optical transparency, good flexibility and robustness. Furthermore, PVC has a low Raman cross-section, which gives clear SERS background signals.[24] Au@Ag-NCs would slowly rise to the water−-cyclohexanone interface and self-assemble into orderly layers under gentle stirring. In the meantime, a newborn thin PVC film was being formed at the water/cyclohexanone interface due to the cyclohexanone evaporation. The PVC film served as a template to fix and support the self-assembled Au@Ag-NCs

DOI: 10.1021/acs.est.7b04327
Environ. Sci. Technol. 2018, 52, 5812−5820

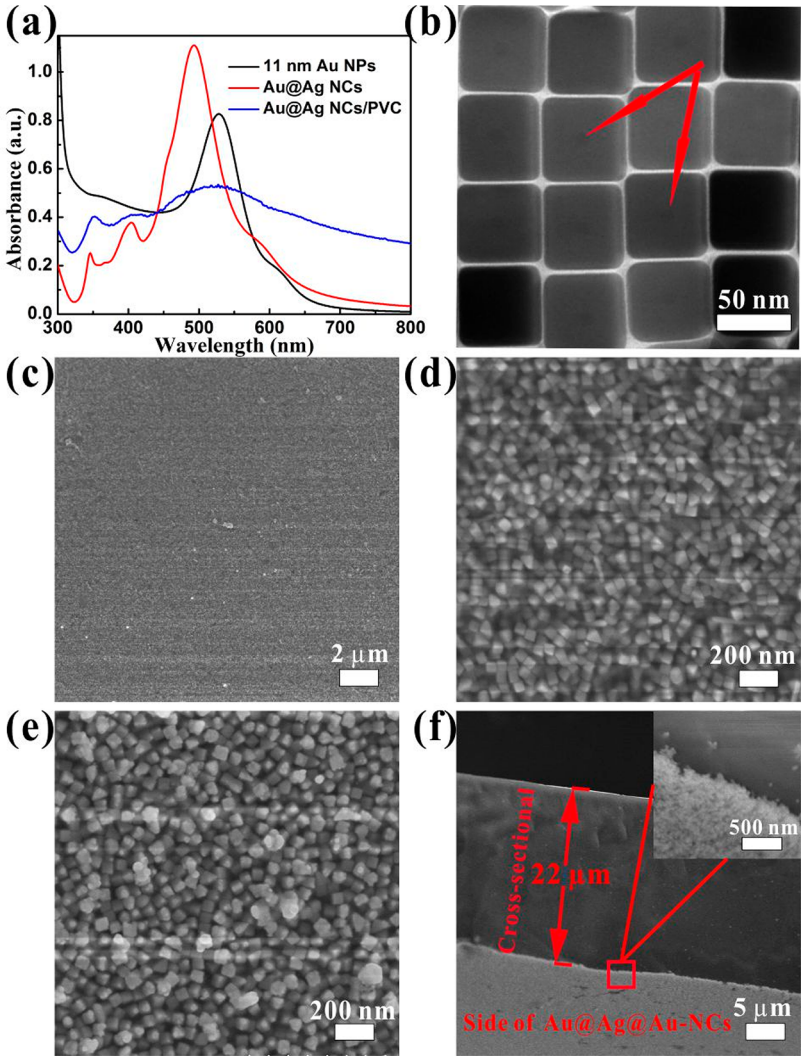

Figure 1. (a) UV−vis spectra of the Au-NPs solution, the Au@Ag-NCs solution, and the Au@Ag-NCs/PVC film. (b) TEM image of the Au@Ag-NCs (the arrows point to the spherical Au-NPs core). (c) Low and (d) high magnification SEM images of the orderly self-assembled Au@Ag-NCs layers. (e) SEM image of the orderly self-assembled Au@Ag-NCs layers after Au coating. (f) Cross-sectional SEM image of the Au@Ag@Au-NCs/PVC film. (inset) Magnified cross-sectional SEM image.

layers. To prevent the oxidation of Ag and prolong its life, the as-prepared Au@Ag-NCs/PVC film was further coated with a thin Au-film by dipping it in a $HAuCl_4$ solution for 30 s.[22,23] Finally, the Au@Ag@Au-NCs/PVC film was obtained.

3.2. Characterization of the Au@Ag@Au-NCs/PVC Film: Microstructure and Morphology. Au@Ag-NCs were synthesized by depositing Ag on the as-prepared Au-NPs. As shown in Figure 1a, the as-prepared Au-NPs have a strong absorption characteristic band with a peak at wavelength of 520 nm. After Ag deposition on Au-NPs, the UV−vis spectrum of Au@Ag-NCs blue shifts to 490 nm (Figure 1a).[21] The SEM observation reveals that the Au@Ag-NCs are uniform nanocubes with an average diameter of 50 nm (Figure S2), which favors for the formation of well-ordered close-packed layers. The TEM observation (Figure 1b) suggests that each Au@Ag-NCs consists of a spherical Au-core (11 nm) and a Ag-shell ~20 nm thick. Compared to the Au@Ag-NCs solution, the absorption peak of the Au@Ag-NCs/PVC film exhibits a red shift from 490 to 514 nm. The red shift may be due to the stronger plasmonic coupling between adjacent Au@Ag-NCs, indicating the formation of assembled Au@Ag-NCs layers on the PVC template. SEM examination (Figure 1c) shows that numerous Au@Ag-NCs are closely packed into 2D layers on the PVC template surface. No obvious gap is seen over a large area (>400 μm^2), suggesting a good uniformity of the Au@Ag-NCs/PVC film, thus ensuring highly repeatable SERS measurement results. The high magnification SEM images (Figures 1d and S3a) show that uniform 50 nm Au@Ag-NCs self-assemble into highly serried layers and the average gap between the adjacent Au@Ag-NCs is less than 10 nm, implying that these small gaps act as highly effective hot spots for remarkable SERS signal enhancement. Although Au@Ag-NCs are able to yield high signal enhancement factor, they are not suitable for long-term use as Ag is easily to be oxidized intrinsically. Thus, the Au@Ag-NCs/PVC film was further coated with a thin Au film to prevent Ag oxidation and prolong its operational life span.[22,23] After Au coating, the Au@Ag-NCs became slightly bigger and some small bright spots appeared (Figures 1e and S3b). These spots may be due to a higher deposition of Au (see details in Table S1 and Figure S4 in the Supporting Information). A long-term test was carried out to evaluate the stability of the Au@Ag@Au-NCs/PVC film. The

DOI: 10.1021/acs.est.7b04327
Environ. Sci. Technol. 2018, 52, 5812−5820

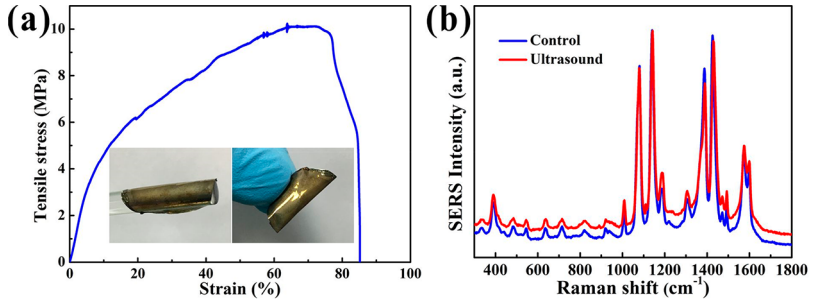

Figure 2. (a) Stress−strain curve of the Au@Ag@Au-NCs/PVC film. (inset) Digital photographs of the Au@Ag@Au-NCs/PVC film wrapping around a glass rod and folded by hand. (b) SERS spectra of 4-ATP collected from the Au@Ag@Au-NCs/PVC film before and after ultrasonication. Experimental conditions: laser power = 0.04 mW; integration time = 10 s.

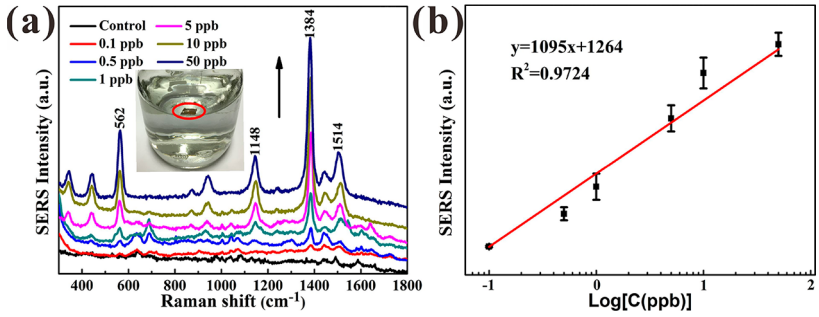

Figure 3. (a) SERS spectra collected from the Au@Ag@Au-NCs/PVC film which floated on the water surface with various thiram concentrations. (inset) Digital photograph of the Au@Ag@Au-NCs/PVC film floating on the surface of water. (b) Quantitative calibration curve of SERS peak intensities at 1384 cm^{-1} against the natural logarithm over their concentrations. Error bars represent the standard errors of three identical SERS measurements. Experimental conditions: laser power = 0.04 mW; integration time = 10 s.

result demonstrated that the intensity of SERS peaks of the Au@Ag-NCs/PVC film reduced about 30% after 1 month of storage (Figure S5a), probably due to the Ag oxidation, whereas no obvious decrease in the intensity of SERS peaks of the Au@Ag@Au-NCs/PVC film was observed (Figure S5b), suggesting that it is more stable and could be kept in storage for longer time.

Since the Au@Ag@Au-NCs/PVC film is composed of the assembled Au@Ag@Au-NCs layer and the PVC supporting layer, the thickness of the SERS-active layer can be easily tuned by adjusting the Au@Ag-NCs dosage and the flotation time, while the thickness of the PVC layer was facilely controlled by the PVC dosage (2−15 mg/cm^2). As Au@Ag-NCs are not optically transparent, the thickness of the assembled Au@Ag-NCs has to be optimized to allow light penetration and escape of Raman-scattered photons and maximize Raman SERS signals. The results suggest that the number of assembled Au@Ag@Au-NCs layers should be less than five to allow enough light to pass through (Figure S6). Considering ease of practical applications, such as storage, transportation, and floating conditions on the water surface, the Au@Ag@Au-NCs/PVC film is designed to be as light and flexible as possible while still self-supportive. Hence, the PVC dosage was optimized to be 5 mg/cm^2. The cross-sectional SEM image (Figure 1f) shows that the Au@Ag@Au-NCs/PVC film is only 22 μm thick when PVC dosage is 5 mg/cm^2, while the assembled Au@Ag@Au-NCs layer is less than 0.3 μm thick (the inset of Figure 1f). As the assembled Au@Ag@Au-NCs layer was very thin, the supportive PVC contributed to the most weight of the film, thus, the weight per square centimeter of the film was determined by the original PVC dosage, which was ca. 5 mg/cm^2. In summary, the as-prepared Au@Ag@Au-NCs/PVC film is ultrathin and ultralight, thus, highly suitable for storage and transportation in practical applications.

3.3. Characterization of the Au@Ag@Au-NCs/PVC Film: Mechanical Property. To be used in practical applications, such as detection of nonplanar objects, robustness and flexibility are the two most important characteristics required for SERS substrates.[17] Herein, the typical stress−strain testing of the Au@Ag@Au-NCs/PVC film was performed. Figure 2a shows that the Au@Ag@Au-NCs/PVC film possesses a fairly high tensile strength of 10 MPa, while it still exhibits a high elongation at break (>70%). Besides, the film can also be easily wrapped around a glass rod or even folded by hand (Figure 2a inset). These results indicate that the film is robust and flexible. In order to better test the robustness of the Au@Ag@Au-NCs/PVC film, the film was subjected to ultrasonication for 30 min (see Movie 1). It was found that the Au@Ag@Au-NCs layer retained its orderly assembled structure after the ultrasonication, which is significantly better than that of the Au@Ag-NCs layer assembled on the surface of a glass lid or Si wafer (Figure S7a).[19] SEM observation further reveals that the assembled Au@Ag@Au-NCs attached on the PVC film surface have no noticeable defects (Figure S7b). SERS spectra of 4-ATP collected from the Au@Ag@Au-NCs/PVC film indicate that the film can maintain the original SERS enhancement performance after ultrasonication (Figure 2b). The excellent robustness of the film can be attributed to the use of PVC, which can firmly fix the assembled Au@Ag-NCs. Furthermore, PVC, having good elasticity, can provide excellent buffer under the severe vibration by ultrasound. Compared to other traditional substrates, the Au@Ag@Au-NCs/PVC film has astonishing flexibility and robustness, which can keep the nanostructure intact even under strong external force.

DOI: 10.1021/acs.est.7b04327
Environ. Sci. Technol. 2018, 52, 5812−5820

3.4. Characterization of the Au@Ag@Au-NCs/PVC Film: SERS Property. It is critical to assess the reproducibility of SERS signals collected from the Au@Ag@Au-NCs/PVC film for practical application. The Au@Ag@Au-NCs/PVC film was immersed in 4-ATP solution to obtain a monolayer of 4-ATP on the film surface. SERS spectra of the film were collected from 12 randomly selected positions as demonstrated in Figure S8. The result shows that the obtained SERS signal intensities of 4-ATP are highly uniform, and the relative standard deviation of the SERS signal intensities is less than 20%,[25] suggesting Raman enhancement factors (EF) at different sites of the Au@Ag@Au-NCs/PVC film are almost the same. Raman EF was estimated to be $(1.1 \pm 0.2) \times 10^6$ using the reported protocol (see details in section 1 in the Supporting Information). The good reproducibility of SERS signals is attributed to the highly ordered Au@Ag@Au-NCs SERS active layers on the PVC film surface (Figure 1e). Hence, the Au@Ag@Au-NCs/PVC film can provide reliable SERS measurement and be used as a quantitative tool for rapid contaminant detection.

3.5. SERS Analysis: Detection of Contaminants in Aqueous Environments. To tackle random illegal discharge to natural water bodies, it is essential to develop on-site water quality monitoring techniques, especially for the detection of specific contaminants. Owing to its light weight and flexibility, the Au@Ag@Au-NCs/PVC film can easily float on the surface of water and contact with the water without interstices (Figure 3a, inset). Moreover, SERS signals can be directly collected from both sides of the film due to its semioptical transparency, as confirmed by our previous studies.[18] Thus, it is expected that the Au@Ag@Au-NCs/PVC film can serve as a SERS substrate for on-site monitoring of specific contaminants in water.

Pesticide contamination of surface waters has become an issue of concern due to its widespread use.[26] More than 3 million tons of pesticides are produced and consumed annually.[4] These pesticides can easily enter environmental water bodies by runoff, leaching, careless disposal of empty containers, and so on, leading to the poisoning of 3 million people every year.[4] Thus, on-site monitoring of pesticides in aquatic systems is vital to prevent the threats to human health.

Thiram, a typical sulfur-containing pesticide widely used to deal with weeds and apple anthrax, is chosen as a model contaminant in this study.[26] Figure 3a shows the SERS spectra obtained from the Au@Ag@Au-NCs/PVC film in contact with thiram aqueous solutions with different concentrations. There are several characteristic peaks assigned to thiram, such as 562, 1148, 1384, and 1514 cm^{-1}, which are attributed to υ(S−S), $\rho(CH_3)$ or υ(C−N), $\rho(CH_3)$, and υ(C−N), respectively.[27] The strongest peak at 1384 cm^{-1} can be clearly detected even at a very low level of thiram (0.1 ppb). With the increment in thiram concentration, the SERS signal intensity increases proportionally. The reason for the plateau may be that when the thiram concentration is higher than 50 ppb, the SERS-active layer may be fully saturated, thus the SERS intensity would not further increase. The most prominent peak at 1384 cm^{-1} is selected as the indicator, as it is the most sensitive peak when thiram concentration is lower than 50 ppb. Figure 3b shows that the peak intensity of 1384 cm^{-1} is proportional to the corresponding natural logarithm of thiram concentration ranging from 0.1 to 50 ppb. A satisfactory linear relationship is obtained with the correlation coefficient of 0.972 (Figure 3b). Moreover, the detection limit is 0.1 ppb, which is much lower than those reported previously (See Table 1).

Table 1. Samples for SERS Application in Thiram Detection

SERS substrate	sensitivity	ref
Ag nanoshells	24 ppb (10^{-7} M)	28
Au@Ag NPs	0.24 ppb (10^{-9} M)	27
optofluidic SERS device	5 ppm	29
single clusters of self-assembled Ag NPs	24 ppb	30
gold nanorods	8.16 ppb (34 nM)	31
Au@Ag@Au-NCs/PVC film	0.1 ppb	this study

In consideration of the actual environment applications, we evaluated the performance of the Au@Ag@Au-NCs/PVC film in some extreme conditions, such as strong acid or base, high temperature, and waves. Figure S9 shows that the Au@Ag@Au-NCs/PVC film can still keep its good enhancement performance and on-site contaminant monitoring would not be affected by these harsh environmental conditions (see Movie 2).

The developed Au@Ag@Au-NCs/PVC film was also tested in two environmental water samples, secondary effluent from local wastewater treatment plant and estuary water from Xinglin Bay, to validate its applicability in real application conditions. The results show that SERS characteristic peaks of thiram can still be clearly observed even though the concentration was reduced to 1 ppb in the above two water samples (Figure 4). However, the detection sensitivity and the linear regression coefficients decrease because real water systems are much more complicated; that is, they may contain some interfering species, and the water quality varies with time. In our future work, we would deploy microfluidic platforms, which can separate different components and obtain purer samples,[32,33] to improve the detection sensitivity and accuracy.

To further evaluate the versatility of the Au@Ag@Au-NCs/PVC film, two additional common contaminants (parathion-methyl and MG) were tested in this work. Parathion-methyl, one of the most hazardous insecticides, is widely used to control sucking and chewing insects.[34] MG is a traditional bactericide with high toxicity, which is often illegally added to water bodies to improve the survival rate of fish.[35] The SERS spectra of parathion-methyl and MG aqueous solutions with different concentrations are displayed in Figures S10a and b, respectively. The Raman signal peak of parathion-methyl at 1343 cm^{-1} is distinguishable at the concentration of 100 ppb, while the characteristic Raman signal peak of MG at 1174 cm^{-1} is still visible at a fairly low concentration of 10 ppb. Compared to thiram, the relative lower sensitivities to parathion-methyl and MG are attributed to their weaker affinities to Au or Ag surfaces. To mitigate the problem, the Au or Ag surface should be modified with proper molecules, such as cyclodextrin, to enhance the binding force with the target molecules,[10] which will be studied in our future work. The above results indicate that the Au@Ag@Au-NCs/PVC film can be applied to monitor a range of contaminants.

3.6. SERS Analysis: Feasibility of Illegal Discharge Monitoring. At the beginning of the experiment, SERS peak intensities at 1384 cm^{-1} established a baseline when no thiram was present in the solution, representing uncontaminated river water (Figure 5b). Then, it was observed that the SERS signal intensity suddenly increased when the first injection of thiram solution was conducted (t = 60 min). This injection represents a random illegal discharge, which is hard to capture promptly by conventional monitoring techniques. On the other hand, our method can rapidly pick it up once there is a surge in the contaminant level; that is, SERS characteristic peaks of the

DOI: 10.1021/acs.est.7b04327
Environ. Sci. Technol. 2018, 52, 5812−5820

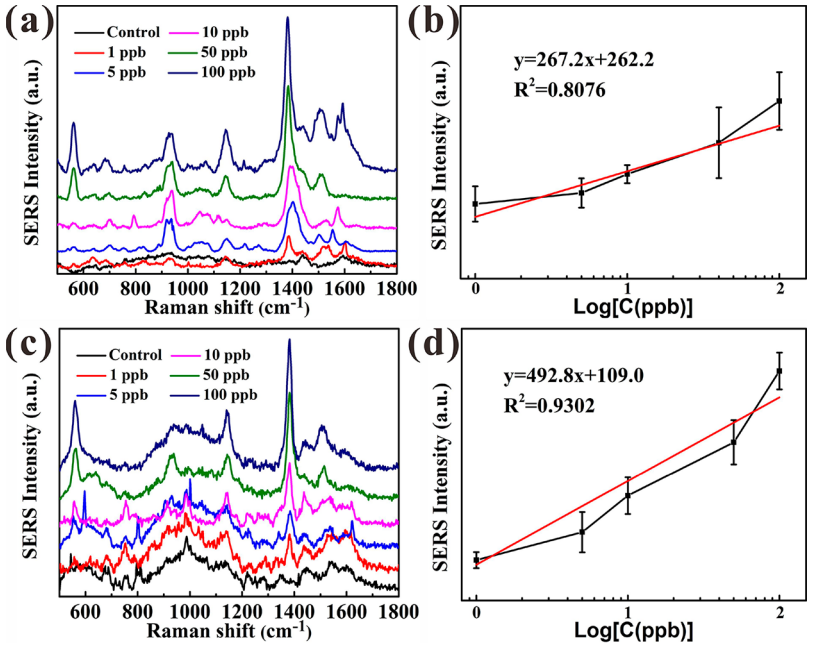

Figure 4. SERS spectra collected from the Au@Ag@Au-NCs/PVC film placed on the surface of (a) the secondary effluent sample from wastewater treatment plant and (c) the estuary water sample. (b and d) Quantitative calibration curve of SERS peak intensities at 1384 cm^{-1} against the natural logarithm over their concentrations according to parts a and c, respectively. Error bar represents the standard error of three identical SERS measurements. Experimental conditions: laser power = 0.02 mW, integration time = 10 s.

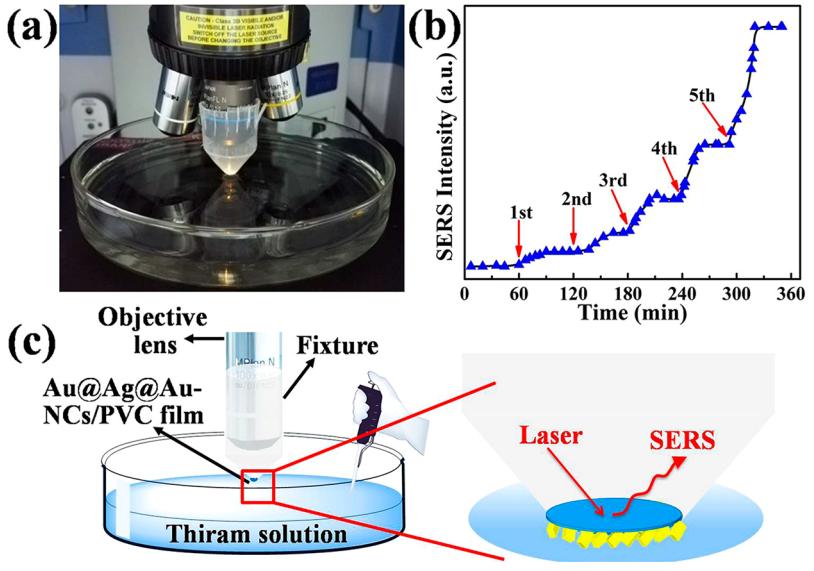

Figure 5. (a) Digital photograph of the simulated illegal discharge monitoring setup (thiram used as a model contaminant). (b) SERS peak intensities at 1384 cm^{-1} collected from the Au@Ag@Au-NCs/PVC film floating on the surface of water samples with five consecutive injections of thiram. Each injection contains 40 μL of 10 ppm thiram solution with an interval time of 60 min. (c) Schematic illustration of simulated on-site monitoring of contaminant in water body. Experimental conditions: laser power = 0.4 mW, integration time = 5 s.

contaminant appear within a few minutes. Most importantly, the method is able to identify contaminants by their distinctive fingerprinting. The simulated monitoring experiments were performed for five consecutive injections of thiram solution with an overall monitoring time of 360 min, and similar changes of SERS signal intensity have been observed, suggesting good stability of the film. As the adsorption of thiram on film was firm, the intensity signals are accumulated. The above results show that illegal discharge monitoring is feasible based on the Au@Ag@Au-NCs/PVC film.

We have also performed a similar experiment using a portable Raman spectrometer for on-site Raman pollutant detection. As shown in Figure S11 (Supporting Information), with an increment in thiram concentration, SERS intensity increases correspondingly, suggesting the possibility of on-site illegal discharge monitoring using the Au@Ag@Au-NCs/PVC film and a portable Raman spectrometer.

3.7. SERS Analysis: Reutilization of the Au@Ag@Au-NCs/PVC Film. An ideal SERS substrate should be reusable in order to effectively reduce the detection cost. Unfortunately, most of the currently reported SERS substrates are difficult to

DOI: 10.1021/acs.est.7b04327
Environ. Sci. Technol. 2018, 52, 5812−5820

clean and are usually disposed after one-time analysis to avoid any contamination from the previous tests.[36] The main reason for this is that strong cleaning agents, which can break the chemical bond between the adsorbed compounds and the SERS-active substrates, are usually required to clean up the compounds adsorbed on the SERS-active substrate, especially those having strong adsorption affinity to the SERS substrate (like thiram). However, as the ordered nanostructure in most SERS substrates are mainly assembled by simple physical adsorption on or chemical interaction with the support template, strong cleaning agents are likely to destroy such nanostructures. On the contrary, since the assembled Au@Ag@Au-NCs layers are firmly fixed on the PVC template in our work, the film can stand strong cleaning agents, as proved in the previous ultrasonication test. Herein, a strong reductant, $NaBH_4$, was used to break the chemical bond between the contaminant and the Au@Ag@Au-NCs surface so that a clean SERS substrate can be obtained.[37] As shown in Figure 6, there

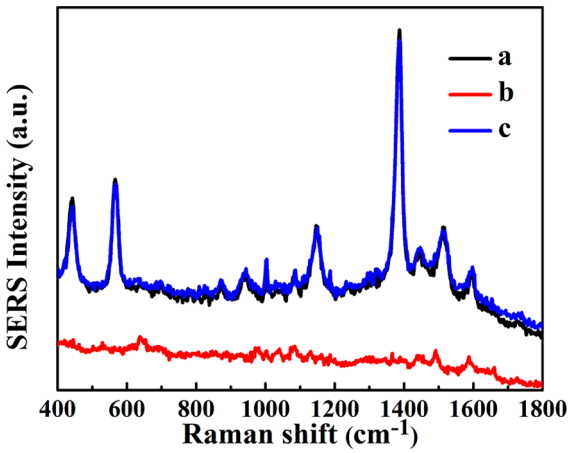

Figure 6. SERS spectra collected from (a) a fresh Au@Ag@Au-NCs/PVC film which floated on 10 ppb thiram solution; (b) sample a after washing with $NaBH_4$; (c) a regenerated Au@Ag@Au-NCs/PVC film which floated on 10 ppb thiram solution. Experimental conditions: laser power = 0.04 mW; integration time = 10 s.

is no obvious Raman peak for the regenerated Au@Ag@Au-NCs/PVC film after $NaBH_4$ cleaning, indicating a complete removal of thiram. Whereas, when the regenerated Au@Ag@Au-NCs/PVC film was reused to detect thiram in water solution, the peak intensity assigned to thiram had no obvious attenuation, suggesting that the film retained high Raman activity after strong chemical cleaning. As the Au@Ag@Au-NCs/PVC film can be easily regenerated, the cost of this method would be greatly reduced, broadening its applications.

4. OVERVIEW AND FUTURE WORK

A flexible, ultralight, and robust substrate was fabricated via interface self-assembly of Au@Ag-NCs on a simultaneously formed PVC template, and a subsequent thin Au-film coating. Due to its flexibility, light weight, and robustness, the Au@Ag@Au-NCs/PVC film is suitable for surface water contaminant detection even in harsh environmental conditions. The detection of a model contaminant (thiram) in both standard water solution and actual aqueous samples was carried out, and the detection limits were 0.1 and 1 ppb, respectively. Simulated experiments illustrated that Raman signals of thiram can be instantly and consecutively detected with the as-fabricated Au@Ag@Au-NCs/PVC film, implying that illegal discharge monitoring is feasible. Furthermore, the Au@Ag@Au-NCs/PVC film could be easily regenerated. In summary, the developed method is facile and inexpensive, which has great potential in on-site pollutant monitoring with the aid of a portable Raman spectrometer. However, further research effort is still required to optimize the current method. First, specialized modifications of the Au@Ag@Au-NCs/PVC film are required to improve its sensitivity and selectivity. Second, self-assembly nanostructure and polymers need to be further finely tuned to achieve better reproducibility and higher enhancement factors. Third, a microfluidic platform can be applied to reduce the disturbance from the interference compounds in real water samples so that better detection sensitivity and accuracy can be achieved. Last, it is anticipated that the interface self-assembly method can also be explored to assemble other nanomaterials and polymers for the fabrication of various flexible devices, such as flexible sensors, electrodes, etc.

■ ASSOCIATED CONTENT

Supporting Information

The Supporting Information is available free of charge on the ACS Publications website at DOI: 10.1021/acs.est.7b04327.

Additional information as noted in text (PDF)
Demonstration of ultrasonication testing (MP4)
Demonstration of conditions testing (MP4)

■ AUTHOR INFORMATION

Corresponding Author

*E-mail: ymzheng@iue.ac.cn. Fax: +86-592-6190977. Tel.: +86-592-6190785.

ORCID

Yu-Ming Zheng: 0000-0002-3858-1037

Notes

The authors declare no competing financial interest.

■ ACKNOWLEDGMENTS

The authors acknowledge the financial support received from the National Natural Science Foundation of China (grant nos. of 21507124, 51578525, 5153000136, and 31400797), the Natural Science Foundation of Fujian Province (No.2015J05036), the Science and Technology Planning Project of Xiamen City (NO.3502Z20162004), and the Hundred Talents Program of the Chinese Academy of Sciences. We also thank Dr. Shaoyang Liu from the Department of Chemistry and Physics, Troy University, for revising the English.

■ REFERENCES

(1) Ali, I. New generation adsorbents for water treatment. *Chem. Rev.* **2012**, *112*, 5073−5091.
(2) Montgomery, M. A.; Elimelech, M. Water and sanitation in developing countries: including health in the equation. *Environ. Sci. Technol.* **2007**, *41*, 17−24.
(3) Shannon, M. A.; Bohn, P. W.; Elimelech, M.; Georgiadis, J. G.; Marinas, B. J.; Mayes, A. M. Science and technology for water purification in the coming decades. *Nature* **2008**, *452*, 301−310.
(4) Schwarzenbach, R. P.; Egli, T.; Hofstetter, T. B.; von Gunten, U.; Wehrli, B. Global water pollution and human health. *Annu. Rev. Env. Resour.* **2010**, *35*, 109−136.

DOI: 10.1021/acs.est.7b04327
Environ. Sci. Technol. 2018, 52, 5812−5820

(5) Schwarzenbach, R. P.; Escher, B. I.; Fenner, K.; Hofstetter, T. B.; Johnson, C. A.; von Gunten, U.; Wehrli, B. The challenge of micropollutants in aquatic systems. *Science* **2006**, *313*, 1072−1077.
(6) Petrie, B.; Barden, R.; Kasprzyk-Hordern, B. A review on emerging contaminants in wastewaters and the environment: current knowledge, understudied areas and recommendations for future monitoring. *Water Res.* **2015**, *72*, 3−27.
(7) Esmaielzadeh Kandjani, A. E.; Sabri, Y. M.; Mohammad-Taheri, M.; Bansal, V.; Bhargava, S. K. Detect, remove and reuse: A new paradigm in sensing and removal of Hg (II) from wastewater via SERS-active ZnO/Ag nanoarrays. *Environ. Sci. Technol.* **2015**, *49*, 1578−1584.
(8) Fang, W.; Zhang, X.; Chen, Y.; Wan, L.; Huang, W.; Shen, A.; Hu, J. Portable SERS-enabled micropipettes for microarea sampling and reliably quantitative detection of surface organic residues. *Anal. Chem.* **2015**, *87*, 9217−9224.
(9) Li, D.; Qu, L.; Zhai, W.; Xue, J.; Fossey, J. S.; Long, Y. Facile on-site detection of substituted aromatic pollutants in water using thin layer chromatography combined with surface-enhanced Raman spectroscopy. *Environ. Sci. Technol.* **2011**, *45*, 4046−4052.
(10) Li, D.-W.; Zhai, W.-L.; Li, Y.-T.; Long, Y.-T. Recent progress in surface enhanced Raman spectroscopy for the detection of environmental pollutants. *Microchim. Acta* **2014**, *181*, 23−43.
(11) Álvarez-Puebla, R. A.; Liz-Marzán, L. M. Environmental applications of plasmon assisted Raman scattering. *Energy Environ. Sci.* **2010**, *3*, 1011−1017.
(12) Halvorson, R. A.; Vikesland, P. J. Surface-enhanced Raman spectroscopy (SERS) for environmental analyses. *Environ. Sci. Technol.* **2010**, *44*, 7749−7755.
(13) Li, N.; Hu, C. Z.; Fu, X. N.; Xu, X. F.; Liu, R.; Liu, H. J.; Qu, J. H. Identification of Al_{13} on the colloid surface using surface-enhanced Raman spectroscopy. *Environ. Sci. Technol.* **2017**, *51*, 2899−2906.
(14) Fu, Y.; Kuppe, C.; Valev, V. K.; Fu, H. B.; Zhang, L. W.; Chen, J. M. Surface-enhanced Raman spectroscopy: A facile and rapid method for the chemical component study of individual atmospheric aerosol. *Environ. Sci. Technol.* **2017**, *51*, 6260−6267.
(15) Guo, H. Y.; Zhang, Z. Y.; Xing, B. S.; Mukherjee, A.; Musante, C.; White, J. C.; He, L. L. Analysis of silver nanoparticles in antimicrobial products using surface-enhanced Raman spectroscopy (SERS). *Environ. Sci. Technol.* **2015**, *49*, 4317−4324.
(16) Ouyang, L.; Li, D.; Zhu, L.; Yang, W.; Tang, H. A new plasmonic Pickering emulsion based SERS sensor for in situ reaction monitoring and kinetic study. *J. Mater. Chem. C* **2016**, *4*, 736−744.
(17) Polavarapu, L.; Liz-Marzan, L. M. Towards low-cost flexible substrates for nanoplasmonic sensing. *Phys. Chem. Chem. Phys.* **2013**, *15*, 5288−5300.
(18) Zhong, L. B.; Yin, J.; Zheng, Y. M.; Liu, Q.; Cheng, X. X.; Luo, F. H. Self-assembly of Au nanoparticles on PMMA template as flexible, transparent, and highly active SERS substrates. *Anal. Chem.* **2014**, *86*, 6262−6267.
(19) Li, Y. J.; Huang, W. J.; Sun, S. G. A universal approach for the self-assembly of hydrophilic nanoparticles into ordered monolayer films at a toluene/water interface. *Angew. Chem., Int. Ed.* **2006**, *45*, 2537−2539.
(20) Duan, H.; Wang, D.; Kurth, D. G.; Mohwald, H. Directing self-assembly of nanoparticles at water/oil interfaces. *Angew. Chem., Int. Ed.* **2004**, *43*, 5639−5642.
(21) Ma, Y.; Li, W.; Cho, E. C.; Li, Z.; Yu, T.; Zeng, J.; Xie, Z.; Xia, Y. Au@Ag core-Shell nanocubes with finely tuned and well-controlled sizes, shell thicknesses, and optical properties. *ACS Nano* **2010**, *4*, 6725−6734.
(22) Gutes, A.; Maboudian, R.; Carraro, C. Gold-coated silver dendrites as SERS substrates with an improved lifetime. *Langmuir* **2012**, *28*, 17846−178450.
(23) Sun, Y. G.; Xia, Y. N. Mechanistic study on the replacement reaction between silver nanostructures and chloroauric acid in aqueous medium. *J. Am. Chem. Soc.* **2004**, *126*, 3892−3901.
(24) Tian, Z. Q.; Ren, B. Adsorption and reaction at electrochemical interfaces as probed by surface-enhanced Raman spectroscopy. *Annu. Rev. Phys. Chem.* **2004**, *55*, 197−229.
(25) Ye, J.; Hutchison, J. A.; Uji-i, H.; Hofkens, J.; Lagae, L.; Maes, G.; Borghs, G.; Van Dorpe, P. Excitation wavelength dependent surface enhanced Raman scattering of 4-aminothiophenol on gold nanorings. *Nanoscale* **2012**, *4*, 1606−1611.
(26) Konstantinou, I. K.; Hela, D. G.; Albanis, T. A. The status of pesticide pollution in surface waters (rivers and lakes) of Greece. Part I. Review on occurrence and levels. *Environ. Pollut.* **2006**, *141*, 555−570.
(27) Liu, B.; Han, G.; Zhang, Z.; Liu, R.; Jiang, C.; Wang, S.; Han, M. Y. Shell thickness-dependent Raman enhancement for rapid identification and detection of pesticide residues at fruit peels. *Anal. Chem.* **2012**, *84*, 255−261.
(28) Yang, J. K.; Kang, H.; Lee, H.; Jo, A.; Jeong, S.; Jeon, S. J.; Kim, H. I.; Lee, H. Y.; Jeong, D. H.; Kim, J. H.; Lee, Y. S. Single-step and rapid growth of silver nanoshells as SERS-active nanostructures for label-free detection of pesticides. *ACS Appl. Mater. Interfaces* **2014**, *6*, 12541−12549.
(29) Yazdi, S. H.; White, I. M. Multiplexed detection of aquaculture fungicides using a pump-free optofluidic SERS microsystem. *Analyst* **2013**, *138*, 100−103.
(30) Yuan, C.; Liu, R.; Wang, S.; Han, G.; Han, M.-Y.; Jiang, C.; Zhang, Z. Single clusters of self-assembled silver nanoparticles for surface-enhanced Raman scattering sensing of a dithiocarbamate fungicide. *J. Mater. Chem.* **2011**, *21*, 16264−16270.
(31) Saute, B.; Premasiri, R.; Ziegler, L.; Narayanan, R. Gold nanorods as surface enhanced Raman spectroscopy substrates for sensitive and selective detection of ultra-low levels of dithiocarbamate pesticides. *Analyst* **2012**, *137*, 5082−5087.
(32) Chrimes, A. F.; Khoshmanesh, K.; Stoddart, P. R.; Mitchell, A.; Kalantar-zadeh, K. Microfluidics and Raman microscopy: current applications and future challenges. *Chem. Soc. Rev.* **2013**, *42*, 5880−5906.
(33) Huang, J. A.; Zhang, Y. L.; Ding, H.; Sun, H. SERS-Enabled Lab-on-a-Chip Systems. *Adv. Opt. Mater.* **2015**, *3*, 618−633.
(34) Li, J. F.; Huang, Y. F.; Ding, Y.; Yang, Z. L.; Li, S. B.; Zhou, X. S.; Fan, F. R.; Zhang, W.; Zhou, Z. Y.; Wu, D. Y.; Ren, B.; Wang, Z. L.; Tian, Z. Q. Shell-isolated nanoparticle-enhanced Raman spectroscopy. *Nature* **2010**, *464*, 392−395.
(35) Sudova, E.; Machova, J.; Svobodova, Z.; Vesely, T. Negative effects of malachite green and possibilities of its replacement in the treatment of fish eggs and fish: a review. *Vet. Med.* **2008**, *52*, 527−539.
(36) Jeong, J. W.; Arnob, M. M.; Baek, K. M.; Lee, S. Y.; Shih, W. C.; Jung, Y. S. 3D cross-point plasmonic nanoarchitectures containing dense and regular hot spots for surface-enhanced Raman spectroscopy analysis. *Adv. Mater.* **2016**, *28*, 8695−8704.
(37) Ansar, S. M.; Ameer, F. S.; Hu, W.; Zou, S.; Pittman, C. U., Jr.; Zhang, D. Removal of molecular adsorbates on gold nanoparticles using sodium borohydride in water. *Nano Lett.* **2013**, *13*, 1226−1229.

DOI: 10.1021/acs.est.7b04327
Environ. Sci. Technol. 2018, 52, 5812−5820